Strategies for modification of titania to harness visible light: A review

Navneet Kaur
Department of Applied Sciences, PEC University of technology

Abstract

Titanium dioxide (TiO_2) is very close to an ideal semiconductor for photocatalysis because of its high stability, low cost and safety toward both humans and the environment. Unfortunately, TiO_2 which is benchmark of UV photocatalysis is inactive under visible light due to their wide band gaps [7,8]. Hence inherent in them is the inability to make use of the vast potential of solar photocatalysis. Various techniques have been employed to make them absorb photons of lower energy as well. These techniques include surface modification via organic materials and semiconductor coupling, band gap modification by creating oxygen vacancies and oxygen sub-stoichiometry, by nonmetals including co-doping of nonmetals and metals doping. The developments made so far through these efforts have been elucidated in this review study. In addition, visible light sensitization of titania by spatial structuring and activation of TiO_2 clusters incorporated in the micropores of zeolite under visible light irradiation by chemical means is also described.

Contents

1. Introduction
2. Structural and Electronic properties of TiO_2
   2.1 Chemical Structure of TiO_2
   2.2 Electronic processes in TiO_2 photocatalysis
   2.3 Recombination
   2.4 Effect of heat treatment on TiO_2
3. Strategies for development of Visible light active titania photocatalysts
   3.1 Dye sensitization
   3.2 Surface-complex assisted sensitization
   3.3 Polymer sensitization
   3.4 Coupled/composite TiO_2
   3.5 Oxygen: vacancies and sub- stoichiometry
   3.6 Defect induced VLA photocatalysis
   3.7 Hybridization
   3.8 Capping
   3.9 Spatially structured and chemically modified VLA titania
   3.10 Oxygen rich TiO_2 modification
   3.11 Band gap modification by doping
   3.12 Doped and coupled TiO_2
4. Current and Future Developments
5. References

---

1. Introduction

The growth of industry worldwide has tremendously increased the generation and accumulation of waste byproducts. In general, the production of useful products has been

focused on and the generation of waste byproducts has been largely ignored. This has caused severe environmental problems that have become a major concern. Researchers all over the world have been working on various approaches to address this issue.

One important technique, called photocatalysis, for removing industrial waste is the use of light energy (electromagnetic radiation) and particles sensitive to this energy to mineralize waste which aids in its removal from solution. It is a catalytic process occurring on the surface of semiconductor materials under the irradiation of photons.[1–5] Photocatalysis involves three processes: the excitation, bulk diffusion and surface transfer of photoinduced charge carriers. These processes are influenced by the bulk structure, surface structure and electronic structure of the semiconductor. Currently the practical applications of this very attractive photocatalytic technique are, however, greatly restricted due to two bottlenecks, which reduce process efficiencies: i.e. narrow light-response range and low separation probability of the photoinduced electron-hole pairs in most stable semiconductor photocatalysts.

The pre-requisite for an efficient photocatalyst is that the redox potential for the evolution of hydrogen and oxygen from water and for the formation of active species like hydroxyl radicals ($OH^{\bullet}$), hydrogen peroxide (H_2O_2) and super oxide ($O_2^{\bullet-}$) should lie within the band gap of a semiconductor photocatalyst [6]. Since photocatalytic reaction proceeds in air saturated and water rich environment, the employed catalyst should remain stable under these conditions.

Titanium dioxide (TiO_2) is considered very close to an ideal semiconductor for photocatalysis because of its high stability, low cost and safety toward both humans and the environment. Unfortunately, TiO_2 which is benchmark of UV photocatalysis are inactive under visible light due to their wide band gaps [7,8]. Hence inherent in them is the inability to make use of the vast potential of solar photocatalysis. Various techniques have been employed to make them absorb photons of lower energy as well. These techniques include surface modification via organic materials and semiconductor coupling, band gap modification by creating oxygen vacancies and oxygen sub-stoichiometry, by nonmetals including co-doping of nonmetals and metals doping. The developments made so far through these efforts have been elucidated in this review study. In addition, visible light sensitization of titania by spatial structuring and activation of TiO_2 clusters incorporated in the micropores of zeolite under visible light irradiation by chemical means is also described.

2. Structural and Electronic properties of TiO_2

2.1 Chemical Structure of TiO_2

TiO_2 belongs to the family of transition metal oxides. There are four commonly known polymorphs of TiO_2 found in nature: anatase (tetragonal), brookite (orthorhombic), rutile (tetragonal), and TiO_2 (B) (monoclinic)[9]. Besides these polymorphs, two additional high-pressure forms have been synthesized from the rutile phase. These are TiO_2 (II) [10] with a PbO_2 structure and TiO_2 (H) [11] with a hollandite structure. In this review, only the crystal structures (Table 1) [12–14] and properties of the rutile, anatase and brookite polymorphs are considered.

Table 1. Crystal structure data of TiO_2

Properties	Rutile	Anatase	Brookite
Crystal structure	Tetragonal	Tetragonal	Orthorhombic
Lattice constant (Å)	a = 4.5936 c =2.9587	a = 3.784 c = 9.515	a = 9.184 b = 5.447 c = 5.154
Space group	$P4_2/mnm$	$I4_1/amd$	Pbca
Molecule (cell)	2	2	4
Volume/ molecule ($Å^3$)	31.2160	34.061	32.172
Density (g cm^{-3})	4.13	3.79	3.99
Ti–O bond length (Å)	1.949 (4) 1.980 (2)	1.937(4) 1.965(2)	1.87–2.04
O–Ti–O bond angle	81.2° 90.0°	77.7° 92.6°	77.0°–105°

1. Rutile: Rutile TiO_2 has a tetragonal structure and contains 6 atoms per unit cell (Figure 1).

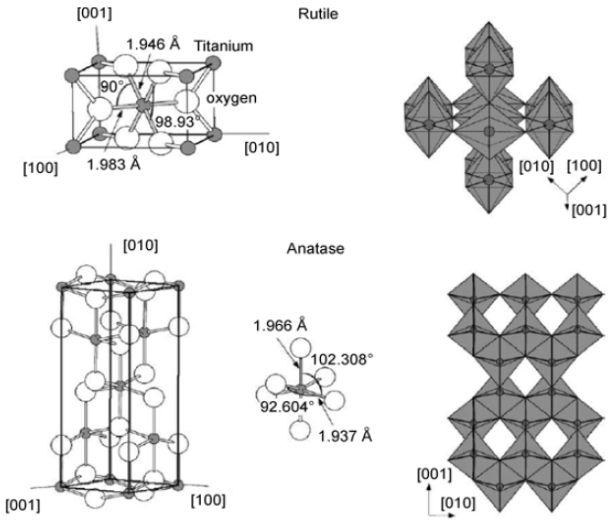

Fig. 1 Crystal structure of rutile and anatase phase of TiO_2

The TiO_6 octahedron is slightly distorted [15–17]. The rutile phase is stable at most temperatures and pressures up to 60 kbar, where TiO_2(II) becomes the thermodynamically favorable phase [18]. Zhang et al. [19] found that anatase and brookite structures transformed to the rutile phase after reaching a certain particle size, with the rutile phase becoming more stable than anatase for particle sizes greater than 14 nm. Once the rutile phase formed, it grew much faster than the anatase. The activity of the rutile phase as a photocatalyst is generally very poor. However, Sclafani et al [20] concluded that the rutile phase can be active or inactive, depending on its preparation conditions.

2. Anatase: Anatase TiO_2 also has a tetragonal structure but the distortion of the TiO_6 octahedron is slightly larger for the anatase phase [21], as depicted in Figure 1. Muscat et al. [22] found that the anatase phase is more stable than the rutile at 0 K, but the energy difference between these two phases is small (~2 to 10 kJ/mol). The anatase structure is preferred over other polymorphs for solar cell applications because of its higher electron mobility, low dielectric constant and lower density [9]. The increased photoreactivity is because of the slightly higher Fermi level, lower capacity to adsorb oxygen and higher degree of hydroxylation in the anatase phase [23]. Selloni [24] reported that the reactivity of (001) facets is greater than that of (101) facets in an anatase crystal. Yang et al. [25] synthesized uniform anatase crystals containing 47% (001) facets using hydrofluoric acid as a morphology controlling agent.

3. Brookite: Brookite TiO_2 belongs to the orthorhombic crystal system. Its unit cell is composed of 8 formula units of TiO_2 and is formed by edge-sharing TiO_6 octahedra. It is more complicated, has a larger cell volume and is also the least dense of the 3 forms and is not often used for experimental investigations [16].

2.2 Electronic processes in TiO_2 photocatalysis

Photocatalysis implies photon assisted generation of catalytically active species rather that the action of light as a catalyst in a reaction [26,27]. If the initial photoexcitation process occurs in an adsorbate molecule, which then interacts with the ground state of the catalyst substrate, the process is referred to as a "catalyzed photoreaction", if, on the other hand, the initial photoexcitation takes place in the catalyst substrate and the photoexcited catalyst then interacts with the ground state adsorbate molecule, the process is a "sensitized photoreaction". In most cases, heterogeneous photocatalysis refers to semiconductor photocatalysis or semiconductor-sensitized photoreactions [28].

In photocatalysis, light of energy greater than the band gap of the semiconductor, excites an electron from the valence band to the conduction band. In the case of anatase TiO_2, the band gap is 3.2 eV, therefore UV light (387 nm) is required. The valence band of TiO_2 is composed of the 2p orbitals of oxygen hybridized with the 3d orbitals of titanium, while the conduction band is only the 3d orbitals of titanium [29]. When TiO_2 is exposed to near-UV light, electrons in the valence band are excited to the conduction band leaving behind holes (h^+), as shown in Figure . The excited electrons (e^-) in the conduction band are now in a purely 3d state and because of dissimilar parity, the transition probability of e^- to the valence band decreases, leading to a reduction in the probability of e^-/h^+ recombination [30].

Electrons in the conduction band can be rapidly trapped by molecular oxygen adsorbed on the titania particle, which is reduced to form superoxide radical anion ($O_2^{\bullet -}$) that may further react with H^+ to generate hydroperoxyl radical ($^{\bullet}OOH$) and further electrochemical reduction yields H_2O_2 [31,32]. These reactive oxygen species may also contribute to the oxidative pathways such as the degradation of a pollutant [31,33,34].

Anatase TiO_2 is considered to be the active photocatalytic component based on charge carrier dynamics, chemical properties and the activity of photocatalytic degradation of organic compounds. It has inherent surface band bending that forms spontaneously in a deeper region with a steeper potential compared with the rutile phase (Figure 2) [35] thus surface hole trapping dominates because spatial charge separation is achieved by the transfer of photogenerated holes towards the surface of the particle via the strong upward band bending. However, in the rutile phase, the bulk recombination of electrons and holes occurs, so only holes very close to the

surface are trapped and transferred to the surface. The absorption of a photon excites an electron to the conduction band (e^-_{CB}) generating a positive hole in the valence band (h^+_{VB}).

$TiO_2 + hv \rightarrow h^+_{VB} + e^-_{CB}$
$e^-_{CB} + h^+_{VB} \rightarrow$ energy
$H_2O + h^+_{VB} \rightarrow {}^{\cdot}OH + H^+$
$O_2 + e^-_{CB} \rightarrow O_2^{\cdot -}$
${}^{\cdot}OH$ + pollutant $\rightarrow \rightarrow \rightarrow H_2O + CO_2$
$O_2^{\cdot -} + H^+ \rightarrow {}^{\cdot}OOH$
${}^{\cdot}OOH + {}^{\cdot}OOH \rightarrow H_2O_2 + O_2$
$O_2^{\cdot -}$ + pollutant $\rightarrow \rightarrow \rightarrow CO_2 + H_2O$
${}^{\cdot}OOH$ + pollutant $\rightarrow CO_2 + H_2O$

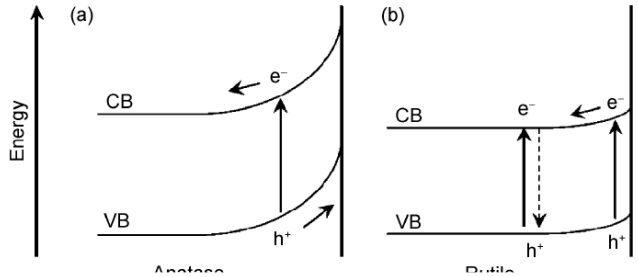

Fig. 2 Surface band bending of the anatase (a) and rutile (b) phases of TiO_2

2.3 Recombination

Recombination of photogenerated charge carriers is the major limitation in semiconductor photocatalysis as it reduces the overall quantum efficiency[26]. When recombination occurs, the excited electron reverts to the valence band without reacting with adsorbed specie [36] non-radiatively or radiatively, dissipating the energy as light or heat [37,38].

Recombination may occur either on the surface or in the bulk and is in general facilitated by impurities, defects, or all factors which introduce bulk or surface imperfections into the crystal [26,39]. Serpone et al., found that trapping excited electrons as Ti^{3+} species occurred on a time scale of ~ 30 ps and that about 90 % or more of the photogenerated electrons recombine within 10 ns [34]. Doping with ions, heterojunction coupling and nanosized crystals have all been reported to promote separation of the electron-hole pair, reducing recombination and therefore improve the photocatalytic activity. For example, the TiO_2 crystallites of Evonik (Degussa) P25 contain a combination of anatase (~80%) and rutile (~20%). The conduction band potential of rutile is more positive than that of anatase which means that the rutile phase may act as an electron sink for photogenerated electrons from the conduction band of the anatase phase. Many researchers attribute the high photocatalytic activity of this preparation to the intimate contact between two phases, enhancing separation of photogenerated electrons and holes, and resulting in reduced recombination [40].

2.4 Effect of Heat treatment on TiO_2

Heat treatment has a vital role in the synthesis of particles, affecting morphology, crystallinity and porosity, and causing a decline in surface area, loss of surface hydroxyl groups and inducing phase transformation. At high temperatures, (400°C and above) the removal of organic materials takes place. The surface area of TiO_2 decreases with calcination time and heating rate because of the collapse of pores in the TiO_2 powder caused by the transformation of amorphous TiO_2 to the anatase phase. Slow heating rates provide relatively mild conditions for phase transformation[41].

Hu et al. [42] have reported that TiO_2 normally undergoes an anatase-to-rutile phase transformation in the range from 600–700°C. The transformation was also affected by factors such as preparation conditions, precursors, impurities, oxygen vacancies and the primary particle size of the anatase phase.

Wang et al. [43] investigated the relationship between the phase transformation and photocatalytic activity of nanosized anatase powder and found that the highest photocatalytic activity for the degradation of acid red B under irradiation with visible light occurred when the rutile phase was on the point of appearing. TiO_2 containing both the rutile and anatase phases enhanced the effect of absorbed visible light than either of the pure phases. Once the rutile phase TiO_2 formed separately, the photocatalytic activity began to decrease rapidly.

Ohtani et al. [44] proposed that TiO_2 with high photocatalytic activity could be achieved by fulfilling two requirements, namely, a large surface area for adsorbing substrates and high crystallinity to reduce the rate of photoexcited e^-/h^+ recombination. Crystallinity increases and the surface area decreases with calcination temperature. The two requirements are partially satisfied at a moderate calcination temperature. Photocatalytic activity per unit mass of TiO_2 bulk reached a broad maximum at a calcination temperature of around 400°C.

Yu et al. [45] showed that the duration of heat treatment also affected the photocatalytic activity of TiO_2 films. When TiO_2 films were heat-treated at 500°C, the rate constant first increased as the heat treatment time lengthened, reached a maximum after 60 min and then decreased upon further heat treatment.

3. Strategies for development of Visible Light Active (VLA) titania photocatalysts

These strategies include various kinds of surface and band modifications that lead to formation of TiO_2

3.1 Dye sensitization

Surface sensitization of a wide band gap semiconductor photocatalyst such as TiO_2 via chemisorbed or physisorbed dyes can increase the efficiency of the excitation process and expand the wavelength range of excitation for the photocatalyst. This occurs through excitation of the sensitizer followed by charge transfer to the semiconductor. Charge carriers can form in semiconductor particles by exciting a dye attached to the surface of the photocatalyst. The excited state can inject either a hole, or more commonly, an electron to the particle. Highly efficient charge injection is observed when a monolayer of a dye is dispersed on a photocatalyst with a high surface area. This sensitization increases the range of wavelength response of the photocatalyst, which is very important for photocatalyst to operate under natural sunlight.

The mechanism of dye sensitization involves exciatation of surface adsorbed dye molecules upon illumination by visible light and inject electrons into the conduction band (CB)

of host semiconductor. According to most of the reports, this injection is favorable due to the more negative potential of the lowest unoccupied molecular orbital (LUMO) of the dye molecules as compared to the conduction band potential of TiO_2 (Fig. 3).

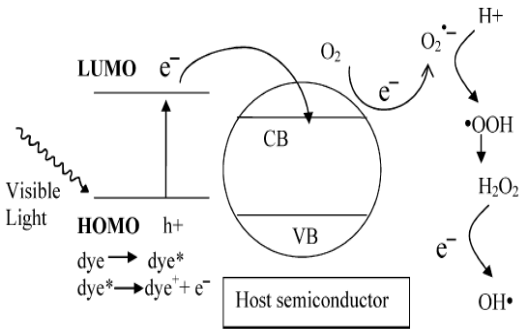

Fig. 3 Visible light activation of a wide band gap semiconductor by dye sensitization

However, an exact location of these molecular orbitals of the dyes with respect to the CB of TiO_2 needs to be mentioned to support the proposed mechanism of electron transfer. The electrons injected by dye molecules hop over quickly to the surface of titania where they are scavenged by molecular oxygen to form superoxide radical $O_2^{\bullet-}$ and hydrogen peroxide radical $^{\bullet}OOH$.

$$e^- + O_2 \rightarrow O_2^{\bullet-}$$

$$O_2^{\bullet-} + H^+ \rightarrow {}^{\bullet}OOH$$

The electron injection and back electron-transfer rates from the dye to the photocatalyst depend upon the nature of the dye molecules, properties of the TiO_2 nanoparticles and the interactions between the dye and nanoparticles [46].

These photoactive radicals decolorize and mineralize substrate dyes by destroying their chromophore structure [47,48,49]. For organic pollutants other than dyes, these radicals attack their aromatic rings forming intermediates and mineralizing them to carbon dioxide and water. The adsorbed dye gets oxidized upon electron injection to the CB of TiO_2 but they are reduced back to their original oxidation state either by accepting electrons from electron donor like aqueous triethanolamine solution (TEOA aq.) or from adsorbed pollutants [47,48,50]. In case of MB, oxidation of the dye follows the reduction process [48].

The extent of dye adsorption depends on the initial dye concentration [51], nature of the dye, surface area of photocatalyst and pH of the solution [51,52]. pH of the solution determines the surface charge of the photocatalyst. Adsorption of the dye is minimum at the pH of the solution where the surface of the photocatalyst carries no electric charge (isoelectric point or point of zero charge). The surface of the photocatalyst is positively charged below isoelectric point and carries a negative charge above it. Depending on the nature of dye that needs to be adsorbed on the surface of a photocatalyst, the adsorption can be low or high in acidic and basic media [52]. For instance, adsorption of acid dyes such as eosin and acid red 44 is favorable at pH below isoelectric point. Higher the surface area of the photocatalyst, higher will be the adsorption sites for the dyes. The visible light activity of reactive red dye 198 sensitized TiO_2 increased upon ultrasonication which deagglomerated titania particles increasing surface active sites for dye or substrates adsorption [51].

Unlike UV photocatalytic process, where an e^-h^+ pair is generated in the wide band gap semiconductor, in dye sensitized visible light photocatalysis no hole exists in the valence band of

the semiconductor corresponding to injected electrons in the CB and therefore no change in pH of the solution is observed with the course of photocatalytic reaction under visible light irradiation [52]. Owing to the high concentration of pollutant in comparison to the adsorbed dye the self-degradation of the adsorbed dyes is kinetically unfavorable in the presence of pollutants. The dyes themselves are attacked by the active species after the pollutants have been degraded [48,51].

Dye sensitized TiO_2 shows appreciable visible light activity only until the adsorbed dye is itself not degraded. It is therefore not a reusable photocatalyst. Dye sensitization is a powerful technique to make TiO_2 sensitive to visible light but frequent desorption of dye molecules significantly reduces the potential use of this technique for practical applications. To avoid desorption, eosin-Y dye has been chemically affixed to platinized TiO_2 particles through silane coupling reagent [50]. Although this chemical fixation prevents photobleaching of eosin-Y but silane coupling reagent hinders electron transfer process from excited dye to CB of TiO_2. The visible light activity of chemically fixed dye thereby remains lower than that of physically mixed system of dye and Pt/titania [50].

Nishikiori et al. [53] found that an increase in the overall crystallinity of TiO_2 nanoparticles increased the surface quality of the nanoparticles, which improved the anchoring geometry of the dye on their surfaces and led to faster electron injection. However, back electron transfer via recombination with oxidized dye molecules, which decreases the quantum yield of photon-to-current conversion, was also enhanced as the crystallinity of the TiO_2 nanoparticles was increased. Amorphous TiO_2 containing some alkoxide groups causing defects inside and outside the amorphous particle-like units served as trapping states with long lifetimes for electrons injected from the excited dye molecules, giving a relatively slow recombination rate. After increasing the crystallinity of the TiO_2 particles, the trapping states were mostly eliminated [54] and surface states formed that increased the rate of back electron transfer to the oxidized dye.

Li et al. [55] reported efficient photocatalytic decomposition of 2,4-dichlorophenol (2,4-DCP) under visible light irradiation by TiO_2 using xanthene dye as a sensitizer. The efficiency of decomposition of 2,4-DCP by TiO_2 sensitized with various dyes decreased in the following order: eosin Y ≈ rose bengal > erythrosine > rhodamine B.

3.2 Surface-complex assisted sensitization

In surface modification techniques like dye sensitization, desorption of dye molecules can severely affect the visible light activity of the photocatalyst [56]. Surface-complex assisted sensitization has proved to be a much better alternative to dye sensitization in this respect. In this technique a surface complex is formed between organic compounds (other than the dyes) and the host photocatalyst via strong chemical bonds [56–58]. This surface complex is sensitive to visible light and injects electrons into the CB of the host semiconductor as illustrated in Fig. 4. The rest of the mechanism is the same as that of dye sensitization.

Li et al. [57] proposed two different surface complexes to explain the observed visible light activity of anatase titania nano particles. The surface complex formed due to the condensation reaction between the hydroxyl group of adsorbed substrate (phenol, 4- chlorophenol (4-CP), 4-hydroxybenzoic) and Ti^{4+}-OH acted as sensitizer to visible light whereas the complex Ti^{4+}-OCR formed due to the reaction between organic moieties formed by autoclaving and Ti^{4+}-OH, trapped these injected electrons [57]. Stepwise removal of the Ti^{4+}-OCR complex by annealing led to a decline in visible light activity. Free hydroxyls on the surface of TiO_2 formed a surface

complex with –NCO groups of tolylene diisocyanate (TDI) via a strong –NHCOOTi chemical bond [56,58]. With an increase in TDI content, visible light absorption by the surface complex formed in case of TDI-modified TiO_2 increased accompanied by a faster rate and higher extent of MB degradation [56].

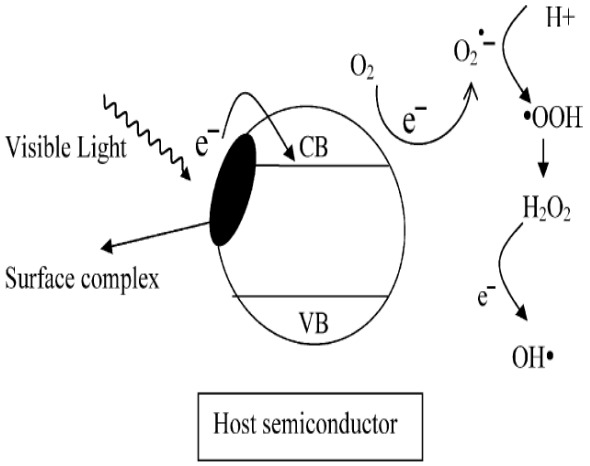

Fig. 4. Visible light activation of a wide band gap semiconductor with surface complex assisted sensitization.

3.3 Polymer sensitization

Both ZnO and TiO_2 have been surface sensitized with conjugated polymer poly(fluorine-co-thiophene) (PFT) instead of a dye resulting in light absorption up to 500 nm wavelength [59,60]. The conjugated polymer PFT plays the same role as that of a dye in dye sensitization. The reductive potential of PFT is weaker than that of TiO_2 and promotes injection of its excited electrons to the conduction band of these semiconductors [59,60]. Polymers are stable sensitizers in water compared to dyes because of their low solubility in water. This is why much higher degradation rate of phenol with TiO_2/PFT is observed than with TiO_2/rhodamine B [59].

3.4 Coupled/composite TiO_2

TiO_2 has been coupled with narrow band gap semiconductor like Bi_2S_3 [61], CdS [61–63], CdSe [64] and V_2O_5 [65] which are capable of absorbing visible light. The basic principle of this technique is similar to dye sensitization except that instead of an organic dye the sensitizer is a narrow band gap semiconductor. The sensitizer semiconductor absorbs visible light and injects electrons into the CB of titania which remains inactive with visible light. These injected electrons can move to the surface of TiO_2 particles and engage to produce active oxidative species as can be seen in Fig. 5.

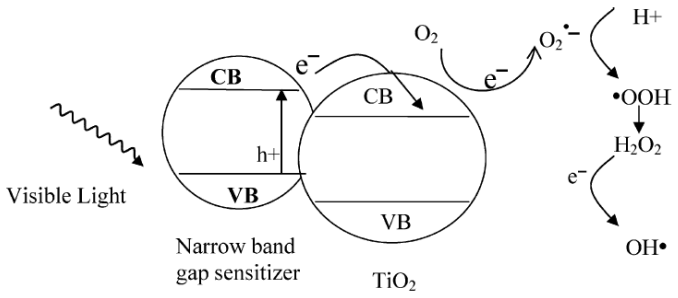

Fig. 5 Visible light activation of TiO_2 by coupling with a narrow band gap semiconductor

The efficient electron and hole transfer between the sensitizer and TiO_2 depends on the difference between the respective conduction band and valence band potentials of the two semiconductors respectively [61,64]. The conduction and valence band potentials of TiO_2 should be more negative and less positive respectively than that of the sensitizer. Alternatively, the CB of narrow band gap semiconductor should be higher than that of titania and its valence band (VB) need to be lower than that of TiO_2 [61,64]. The greater the difference in the band potentials of the two semiconductors, higher is the interfacial charge transfer and vice versa. In addition to the proper location/difference of the band edges of two coupled semiconductors, the extent of visible light absorption of the sensitizer is also crucial for deciding the observed visible light activity of coupled semiconductors.

Similar to dye sensitization, the amount of the narrow band gap semiconductor in contact with TiO_2 surface determines the visible light activity of this coupled system. Both visible light absorption and degradation of MB with composite CdS/TiO_2 nanoparticles under visible light irradiation enhanced with an increase in the CdS content [62]. However, with higher concentration of the sensitizer the surface of the host semiconductor can be covered entirely inhibiting surface redox reactions.

By coupling titanium dioxide with a narrow band gap semiconductor, its photoresponse is extended to the visible region and charge carrier separation is achieved [61–65]. In coupled semiconductors, the VB of sensitizer is higher than that of titania which prevents promotion of visible light generated holes in the VB of sensitizer to the VB of titania extending charge carriers lifetime [61–65]. Under UV–vis irradiation both semiconductors are active. This results in an increase in electron population in the CB of TiO_2 in which electrons are injected not only from the sensitizer but also excited from its own VB. TiO_2 can transfer its photo generated holes to the sensitizer increasing the hole concentration in the VB of sensitizer [61]. This accumulation of charge carriers increases the probability of electron–hole recombination which can significantly reduce the photocatalytic activity of coupled system. Since holes are left behind in the valence band of narrow band gap semiconductors they can photocorrode it if not engaged in redox reactions. Photocorrosion of CdS to Cd has been reported for CdS/TiO_2 system when irradiated with visible light [62]. To prevent photocorrosion of CdS, Ji et al. used sulfite/sulfide which acted as electron donors [63]. High hydrogen production was achieved from seawater over CdS/TiO_2 nanocomposite in the presence of this sacrificial reagent [63].

3.5. Band gap modification by creation of oxygen vacancies and oxygen sub-stoichiometry

TiO_2 is reported to absorb visible light via artificially created oxygen vacancies in its crystal structure [66,67]. Nakamura et al. generated oxygen vacancies in TiO_2 by plasma treatment through radio-frequency discharge [66]. According to Ihara et al. [67], the oxygen vacancies can be easily created in the grain boundaries of the polycrystalline samples which form a grain boundary defect state in the band gap of titania. Oxygen vacancies facilitate visible light absorption by generating discrete states about 0.75 eV and 1.18 eV below the conduction band of TiO_2 [66]. Oxygen vacancies are active electron traps. Since the oxygen defect states lie close to the CB of titania, the electrons captured by oxygen defects can be promoted to the surface by visible light absorption where they engage in degradation of pollutants [66].A decline in the reflectance from 380 to 550nm was noted for oxygen deficient TiO_2 samples [67] while the photoresponse extended to about 600 nm for plasma treated TiO_2 [66]. Justicia et al. [68] observed visible light response with sub stoichiometric TiO2 anatase films. The overlap of defect states generated by oxygen sub-stoichiometry with the CB states of TiO2 reduces its band gap [68].

3.6. Defect induced VLA photocatalysis

VLA titania can also be formed by introducing color centers inside the material [69, 70]. This defect induced doping can be produced either by heat treatment of TiO_2 in vacuum or inert gas environments or by intercalation of small cations (H^+, Li^+ , etc.) into the lattice. In some cases, O_2 is released from the material and Ti^{3+} centers are formed. Very recently, hydrogenation has been demonstrated as a very effective route to engineer the surface of anatase TiO_2 nanoparticles with an amorphous layer which, instead of inducing detrimental recombination effects, resulted in the marked extension of the optical absorption to the infrared range and remarkable enhancement of solar-driven photocatalytic activity [71].

3.7. Hybridization

Conjugated materials are excellent candidates for improving the transportation of photocarriers in photocatalysis by forming electronic interactions with TiO_2 because of its unique electron and hole transport properties. Some efforts have been made to electronically combine conjugated materials with photocatalysts in recent years.

Zhang et al.[72] have demonstrated that surface hybridization of TiO_2 with a few molecular layers of graphite- like carbon yielded an efficient photocatalyst exhibiting photo-induced electrons with high mobility at the graphite- like carbon/TiO_2 interface because of the electronic interactions between the materials. In addition, the response of TiO_2 was extended into the visible range due to the electronic coupling of p states of the graphite-like carbon and conduction band states of TiO_2. TiO_2 with a carbon shell with a thickness of three molecular layers showed a photocatalytic activity that was twice as high as that of Degussa P25 TiO_2 under UV irradiation.

Zhang et al.[73] also obtained an efficient TiO_2 photocatalyst by surface hybridization with a thin layer of C_{60} molecules. The photocatalytic performance of C_{60}-hybridized TiO_2 under UV irradiation was enhanced four times compared with that of a P25-TiO_2 photocatalyst. The increase in photocatalytic activity strongly depended on the coverage of C_{60} molecules on the surface of TiO_2.

Takeuchi et al.[74] prepared various Ti oxide-based photocatalysts such as highly dispersed Ti oxide species within zeolite frameworks, TiO_2 nanoparticles hybridized with

hydrophobic zeolite adsorbents and TiO_2 thin films responsive to visible light. A high photocatalytic reactivity was observed for the photocatalytic decomposition of NO_x and the photocatalytic reduction of CO_2 with H_2O using the TiO_2 semiconducting photocatalysts.

3.8. Capping

The coating of one semiconductor or metal nanomaterial on the surface of another semiconductor or metal nanoparticle core is called capping. Semiconductor nanoparticles are coated with another semiconductor with a different band gap in a core-shell geometry to passivate the surface of the initial nanoparticle and enhance its emissive properties. While the mechanism of charge separation in a capped semiconductor system is similar to that in coupled semiconductor systems, interfacial charge transfer and charge collection in this multicomponent semiconductor system are significantly different. In coupled semiconductor systems, the two particles are in contact with each other and both holes and electrons are accessible for selective oxidation and reduction processes on different particle surfaces. On the other hand, capped semiconductors have a core-shell geometry. By depositing a relatively thick shell of the second semiconductor with a thickness is similar to the core radius it is possible to maintain the individual identities of the two semiconductors. Under these circumstances, only one of the charge carriers is accessible at the surface, while opposite charge transfer to the inner semiconductor occurs, thus improving the selectivity of the interfacial transfer and enhancing the oxidation or reduction reaction [75] (Figure 6). Core-shell geometry has an important consequence in terms of imparting enhanced photo electrochemical stability to the system, taking into account that many of these semiconductors (especially group II–VI compounds) are prone to anodic photocorrosion in aqueous media [76].

Bedja and Kamat[77] prepared TiO_2-capped SnO_2 and SiO_2 colloids. The TiO_2-capped SnO_2 particles were 80 - 100 Å in diameter and exhibited improved photochromic and photocatalytic efficiencies compared with TiO_2-capped SiO_2, TiO_2, SiO_2 and SnO_2 samples. The improved charge separation in this system was confirmed from the enhanced efficiency of hole trapping monitored by the absorption peak at 360 nm. The capped semiconductor system was useful for the oxidation of I– and SCN– and the quantum efficiency for I– oxidation was improved by a factor of 2–3 upon capping SnO_2 with TiO_2.

Sung et al. [78] reported anatase/rutile core-shell structured TiO_2 particles synthesized by controlled heat treatment of poly(ethylene oxide)-TiO_2 hybrid particles.

The mechanism of core-shell structure formation was based upon volume shrinkage, thermal expansion coefficient differences and further decomposition of organic components. These core-shell particles showed enhanced rates of photodecomposition compared with spherical and other commercially available particles, most probably because of the increased surface area of the nanoporous, nanocrystalline structure of the anatase core.

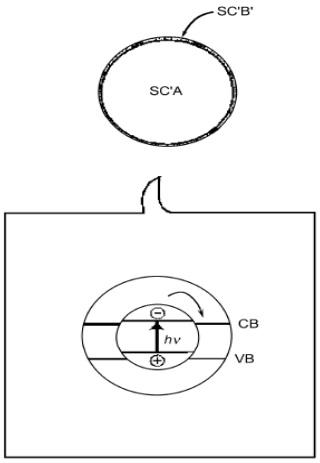

Fig. 6 Electron transfer in a core-shell geometry.

A new series of photocatalysts has been designed by capping noble metal particles of Ag, Au, or Pt [79] with a semiconductor shell. Metal particles with a favorable Fermi level (0.4 V) such as silver and gold are good electron acceptors and facilitate rapid electron transfer from excited TiO_2. The transfer of electrons from the excited semiconductor to the metal is an important aspect that dictates the overall energetics and hence the efficiency of photocatalytic reduction.

Hirakawa et al. [80] reported that Ag core/TiO_2 shell clusters were able to store electrons under UV irradiation and discharge them on demand in the dark. When these clusters were subjected to UV irradiation, a blue shift in the plasmon absorption band from 480 to 420 nm was observed, which reflects an increased electron density in the Ag core during photoirradiation.

Various research groups have studied TiO_2 capped with organic molecules. The photocatalytic investigation of TiO_2 nanocrystals capped with different organic molecules have been performed. The photocatalytic activity of oleic acid- TiO_2 nanocrystals was shown to be even higher than that of Degussa P25 [81]. This behavior indicates a direct involvement of the interface of the materials in photocatalytic reactions.

Fittipaldi et al. [82] carried out multifrequency electron paramagnetic resonance studies on TiO_2 nanocrystals capped with organic moieties prepared by both nonhydrolytic and hydrolytic procedures. The presence of paramagnetic species (carbon radicals) on the surface of the TiO_2 nanocrystals was suggested to account for the high catalytic efficiency of such a nanostructured material.

3.9. Spatially structured and chemically modified visible light active titania

Spatial structuring is a novel physical approach of controlling the size of semiconductor particles from subnanometric to submillimetric length scale[83]. Spatially structured titania photocatalyst in submillimetric length scale can serve as “photonic crystals”. Photonic crystals trap visible photons by increasing the effective light path inside the material which in turn increases the probability of electron excitation owing to longer light/photocatalyst contact time[83]. Highly dispersed and permanently immobilized subnanometric TiO_2 clusters have been formed inside the framework of suchmicroporous hosts as zeolite-Y. The physical approach of spatial structuring of TiO_2 clusters has been respectively integrated with chemical strategies of

dye sensitization [84,85], surfacecomplex assisted sensitization [86] and nitrogen doping to form a bicomponent visible light sensitive and active material. The photoexcited dye ruthenium (II)–tris-bipyridine $[Ru(bpy)_3]^{2+}$ efficiently injects electrons into the conduction band of nearby titania when both of them are incorporated in the supercages of zeolite-Y [84,85]. The organic modifiers such as benzoic acid, 4- aminobenzoic acid and catechol gets adsorbed on the titania cluster encapsulated in zeolite-Y [86]. The titanol group (Ti^{4+}-OH) of these clusters undergo a condensation reaction with adsorbed organic modifies to form a visible light sensitive complex[86]. However, the adsorbed modifiers reduce the volume of zeolite micropores and slow down the diffusion of substrate (phenol) to active titania surface. Self-degradation of these organic modifiers with the reaction course also lowers the activity of these bicomponent systems. In this respect, nitrogen doped titania clusters encapsulated in zeolite-Y is a stable visible light photocatalyst.

3.10. Oxygen rich TiO_2 modification

Recently the visible light active photocatalytic properties have been achieved by the in-situ generation of oxygen through the thermal decomposition of peroxo-titania complex [87]. Increased Ti-O-Ti bond strength and upward shifting of the valence band (VB) maximum were responsible for the visible light activity. The upward shifting of the VB maximum for oxygen rich titania is identified as another crucial reason responsible for efficient visible light absorption. Typical band gap structures of control and oxygen rich titania samples obtained are represented in Figure 7.

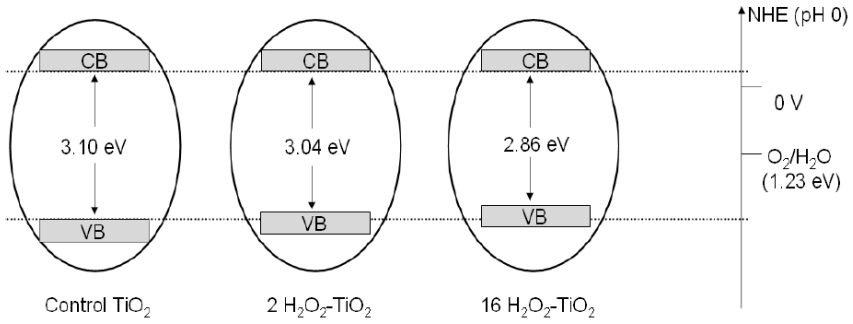

Fig. 7

3.11. Band gap modification by doping

3.11.1 Effect of dopants in the formation of doped TiO_2

Dopants modify the electronic structure of nano-TiO_2 to broaden its effective range of light sensitivity for photocatalysis from the ultra-violet (UV) region to the visible light region[88]. Doping techniques have been shown to be effective and efficient despite their being susceptible to thermal instability and their requirement for expensive ion implantation facilities[89]. Dopants are valued for their ability to confer excellent physicochemical properties such as high crystallinity (high percentage of anatase phase), high specific surface area, and small crystallite size [90, 91].

There are also negative effects of doping techniques in the photocatalytic performance of nano-doped-TiO_2. Firstly, the dopant can act as a charge recombination center that acts against the separation of excited electron and hole. Secondly, doping techniques can inhibit the

production of oxygen radicals in the photocatalysis reaction [92]. However, these problems can be countered by controlling the dosages of the dopants. Besides shifting the wavelength sensitivity of nanodoped- TiO_2 into the visible light range, doping techniques can also improve the physical properties of TiO_2. Cai et al [93, 94] reported that suitable amounts of dopants helps to control the crystallite size of nano-doped-TiO_2 whil producing a high specific surface area of nano-doped-TiO_2. A judicious rate of doping also prevented the transformation of the anatase phase to the rutile phase.

3.11.2 Non metal doping

There are three different main opinions regarding modification mechanism of TiO_2 doped with nonmetals.

(1) Band gap narrowing;
(2) Impurity energy levels; and
(3) Oxygen vacancies.

1. Band gap narrowing: Asahi, et al. [95] found N 2p state hybrids with O 2p states in anatase TiO_2 doped with nitrogen because their energies are very close, and thus the band gap of N-TiO_2 is narrowed and able to absorb visible light.

2. Impurity energy level: Irie, et al. [96] stated that TiO_2 oxygen sites substituted by nitrogen atom form isolated impurity energy levels above the valence band. Irradiation with UV light excites electrons in both the VB and the impurity energy levels, but illumination with visible light only excites electrons in the impurity energy level.

3. Oxygen vacancies: Ihara, et al. [97] concluded that oxygen-deficient sites formed in the grain boundaries are important to emerge vis- activity and nitrogen doped in part of oxygen deficient sites are important as a blocker for reoxidation.

In principle, the strict requirements for anion dopant to elevate the VB maximum are as follows:

i) The electronegativity of the non-metal dopant must be lower than that of oxygen, so that the dopant states can be involved in the formation of a new valence band by locating at its top. Reviewing the Paul's electronegativity of non-metals (B: 2.04; C: 2.55; N: 3.04; O: 3.44; F: 3.98; Si: 1.90; P: 2.19, S: 2.58; Cl: 3.16; Br: 2.96; I: 2.66), it is found that all non-metals except F have lower electronegativities than O and thus have the potential to be of use in allowing visible-light absorption.

ii) The non-metal dopant, as a substitutional lattice atom, should have a radius comparable to that of the lattice O atoms so that the non-metal dopant anions can be uniformly distributed within the whole doped matrix.

It seems that non-metal doping has greater potential for realizing visible-light photoactivity, as already reported. This can be at least partially explained by the following two points:

i) The intrinsic photocatalytic surface properties of a semiconductor still remain well after non-metal doping at the atomic level. In some cases, a more favorable surface structure for photocatalysis may be constructed during surface doping.

ii) The spectral distribution of dopant states is generally located above, but not far from, the VB maximum, which makes the generated holes on these states oxidative enough for subsequent photooxidation reactions.

Nitrogen can be easily introduced in the TiO_2 structure, due to its comparable atomic size with oxygen, small ionization energy and high stability. It was in 1986 when Sato discovered

that addition of NH_4OH in a titania sol, followed by calcination of the precipitated powder, resulted in a material that exhibited a visible light response [98,99]. Later on, Asahi and co-workers explored for first time the visible light activity of N doped TiO_2 produced by sputter deposition of TiO_2 under an N_2/Ar atmosphere, followed by annealing under N_2 [100]. Since then, there have been many reports dealing with nitrogen doping of TiO_2. Significant efforts are being devoted to investigating the structural, electronic and optical properties of N-doped TiO_2, understanding the underlying mechanisms and improving the photocatalytic and self-cleaning efficiency under visible and solar light [101-103]. Comprehensive reviews have been published which summarize representative results of these studies [104,105]. Model pollutants that have been reported to be effectively degraded by VLA photocatalyst include phenols, methylene blue, methyl orange (although dyes have strong absorption in the visible range) and rhodamine B, as well as several gaseous pollutants (e.g., volatile organic compounds, nitrogen oxides).

For the efficient incorporation of nitrogen into TiO_2 either in the bulk or as a surface dopant, both dry and wet preparation methods have been adopted. Physical techniques such as sputtering [106-110] and ion implantation [111,112], rely on the direct treatment of TiO_2 with energetic nitrogen ions. Gas phase reaction methods [113-115], atomic layer deposition [116] and pulsed laser deposition [117] have been successfully applied to prepare N-TiO_2, as well. However, the most versatile technique for the synthesis of N-TiO_2 nanoparticles is the sol–gel method, which requires relatively simple equipment and permits fine control of the material's nanostructure, morphology and porosity. Simultaneous TiO_2 growth and N doping is achieved by hydrolysis of titanium alkoxide precursors in the presence of nitrogen sources. Typical titanium salts (titanium tetrachloride) and alkoxide precursors (including titanium tetra-isopropoxide, tetrabutyl orthotitanate) have been used. Nitrogen containing precursors used include aliphatic amines, nitrates, ammonium salts, ammonia and urea [118-120]. The synthesis root involves several steps; however, the main characteristic is that precursor hydrolysis is usually performed at room temperature. The precipitate is then dried to remove solvents, pulverized and calcined at temperatures from 200 to 600^{o}C.

One promising way to increase the nitrogen content in the TiO_2 lattice is to combine the titanium precursors with a nitrogen-containing ligand, such as Ti^{4+}-bipyridine or Ti^{4+} - amine complexes [121,122]. An alternative soft chemical route is based on the addition of urea during the condensation of an alkoxide acidified solution, leading to interstitial surface doping and shift of the absorption edge well into the visible spectral range (from 3.2 to 2.3 eV) [123]. An innovative sol-gel related technique for the preparation of efficient visible-light active nanostructured TiO_2 is the templating sol-gel method, utilizing titanium precursors combined with nitrogen-containing surfactants. Specifically, successful synthesis of visible light activated N-TiO_2 has been achieved by a simple sol gel method employing dodecylammonium chloride (DDAC) as surfactant [124]. The DDAC surfactant acts simultaneously as a pore templating material to tailor-design the structural properties of TiO_2 (see Figure 3) as well as a nitrogen dopant to induce visible light photoactivity and unique reactivity and functionality for environmental applications[125,126].

In a different approach N-TiO_2, was synthesized via two successive steps: synthesis of TiO_2 and then nitrogen doping using various nitrogen-containing chemicals (e.g. urea, ethylamine, NH_3 or gaseous nitrogen) at high temperatures [127-129] or inductively coupled plasma containing a wide range of nitrogen precursors [130]. In that case, the nitrogen atoms predominantly resided on the TiO_2 surface.

Although most reports on N-TiO_2 concern the anatase polymorphic phase, visible light active N-TiO_2 with anatase-rutile mixed phase (Figure 4) has also been prepared by tuning the parameters of the sol-gel synthesis. Such heterojunction photocatalysts seem to effectively transfer photo-excited electrons from the conduction band of anatase to that of rutile, favoring electron-hole separation and enhancing the visible light photocatalytic activity. [131,132]. Etacheri et al., have successfully developed nitrogen doped anatase rutile heterojunctions which were found to be nine times more photocatalytically active at wavelengths higher than 450 nm (blue filter) in comparison with Evonik P25.

Most of the above methods have also been successfully applied for the doping of 1D titania nanostructures with nitrogen. In this way, N-doped anatase titania nanobelts were prepared via hydrothermal processing and subsequent heat treatment in NH_3 [133]. Similar post-treatment was employed for doping anodized titania nanotubes [134], while high energy ion implantation was found to be more efficient in introducing N atoms in the TiO_2 lattice [135]. Nitrogen localized states have also been introduced into highly ordered TiO_2 nanotubes via nitrogen plasma [136]. Visible light-active N-TiO_2 nanoarray films have also been prepared on sacrificial anodized alumina liquid phase deposition with urea mixed with $(NH_4)_2TiF_6$ aqueous solution [137]. Recently, surface N-doping on titania nanowires, their lateral dimensions reaching the atomic scale, was achieved by the introduction of amines during the condensation stage of the titania precursor [138]. Other approaches for preparing doped TiO_2 nanotubes include employment of nitrogen sources in the electrolyte solutions of electrochemical anodization [139] or in the initial solution of hydrothermal growth [140,141].

3.11.3 Halogen doping

TiO_2 becomes visible light active when doped with halogens like fluorine [142-145] and chlorine [146]. Fluorine atoms easily substitute for O atoms because of their similar ionic radii (1.4A for O_2^- and 1.33A for F^-). Chlorine occupies substitutional as well as interstitial sites in TiO_2 lattice with a charge state of −1 [146]. In fluorine doped titania, fluoride ions have been detected not only at substitutional sites in the lattice but also physically adsorbed on the surface of doped TiO_2 nanoparticles. No shift in the band edge of titania has been observed with fluorine doping since the F 2p states with high density were calculated to appear below the VB maxima. Although fluorine doping does not modify the electronic structure of TiO_2, visible light activity has been observed with F doped TiO_2 samples.

Yamaki et al. [144] suggested that visible light absorption might become possible due to the modification of density of states near the CB edge of rutile TiO_2 with fluorine doping. Fluorine doping generates oxygen vacancies and Ti^{3+} states close to the CBM of TiO_2 which are mainly responsible for the observed visible light activity of the doped samples. Fluorine converts some Ti^{4+} to Ti^{3+} by charge compensation. These Ti^{3+} donor surface states lie below the CB minima like oxygen vacancies states and help trap photogenerated electrons and molecular oxygen to form superoxide radicals. In contrast to fluorine, chlorine doping introduces new levels in the band gap of titania and enables titania to absorb light with wavelengths as high as 700 nm. The photogenerated electrons can make multiple transitions to the CB of titania via intermediate levels.

Chlorine doping lowered the transition temperatures from amorphous to anatase and from anatase to rutile of TiO_2. Fluorine doping on the other hand suppressed the formation of brookite

phase and transformation from anatase to rutile. Contrary to this, fluorine has also been reported to favor formation of rutile phase in TiO_2.

3.11.4 Sulfur doping

Successful insertion of sulfur into the TiO_2 lattice is far more difficult to achieve than nitrogen, due to its larger ionic radius. Insertion of cationic sulfur (S^{6+}) is chemically favourable over the ionic form (S^{2-}) lattice.

Periyat et al., successfully developed S-doped TiO_2 through modification of titanium isopropoxide with sulphuric acid. They found that formation of titanyl oxysulfate results in the retention of anatase at increased temperatures (≥ 800 °C) and that the presence of sulfur causes increased visible light photocatalytic activity of the synthesised materials[147]. Recently, visible light activated sulfur doped TiO_2 films were successfully synthesized using a novel sol-gel method based on the self-assembly technique with a nonionic surfactant to control nanostructure and H_2SO_4 as an inorganic sulfur source [148]. Sulfur species distributed uniformly throughout the films were identified both as S^{2-} ions related to anionic substitutional doping of TiO_2 as well as S^{6+}/S^{4+} cations, attributed mainly to the presence of surface sulfate groups.

3.11.5 Boron doping

Boron doping in TiO_2 shifts its band edge to higher wavelengths and enhances its visible light absorption [149,150]. B doping in titania is reported to extend its visible light absorption to wavelength as high as 800 nm [149].

Zhang and Liu [150] proposed that B doping reduced the band gap of titania by modifying the electronic structure around the conduction band edge.

3.11.6 Carbon doping

Carbon has been incorporated in titania lattice both as an anion [151] and as a cation [152]. The band gap of titania reduces by carbon doping [151–154]. With incorporation of carbon into titania matrix the conduction band edge shifted to reduce the band gap and surface states were introduced near the valence band edge [154]. The electrons excited from these surface states had the potential to form $O_2^{\bullet-}$ and $^{\bullet}OH$ radicals that efficiently mineralized 4-chlorophenol under visible light irradiation [154]. Carbon doping may form carbonaceous species at the surface of TiO_2 which are reported to facilitate in visible light absorption [151,153].However they can lower the photocatalytic activity of C doped TiO_2 samples by covering the surface and blocking surface active sites [151].

3.11.7 Doping with transition metal cations

Transition metal ions can provide additional energy levels within the band gap of a semiconductor. Electron transfer from one of these levels to the conduction band requires lower photon energy than in the situation of an unmodified semiconductor. TiO_2 has been doped with many different transition metals.

Enhancing the rate of photoreduction by doping a semiconductor with metal ions can produce a photocatalyst with an improved trapping-to-recombination rate ratio. However, when metal ions or oxides are incorporated into TiO_2 by doping, the impurity energy levels formed in the band gap of TiO_2 can also lead to an increase in the rate of recombination between photogenerated electrons and holes. Photocatalytic reactions can only occur if the trapped

electron and hole are transferred to the surface of the photocatalyst. This means that metal ions should be doped near the surface of the photocatalyst to allow efficient charge transfer. In the case of doping at a high concentration, metal ions can behave as recombination centers.

Grätzel et al. [155] studied the effect of doping TiO_2 with transition metals such as Fe, V and Mo by electron paramagnetic resonance.

Joshi et al. [156] reported the adverse effect of doping TiO_2 with transition metal ions on photocatalytic activity because of the formation of localized d-states in the band gap of TiO_2. Localized d-states act as trapping sites that capture electrons from the conduction band or holes from the valence band. From a chemical point of view, TiO_2 doping is equivalent to the introduction of defect sites like Ti^{3+} into the semiconductor lattice, where the oxidation of Ti^{3+} species is kinetically fast compared with the oxidation of Ti^{4+}. The differences in photoactivity derive from the change in the diffusion length of the minority carriers [76]. For optimal e^-/h^+ separation, the magnitude of the potential drop across the space-charge layer should not fall below 0.2 V [77]. The dopant content directly influences the rate of e^-/h^+ recombination by the equation: $W = (2\ \varepsilon\varepsilon_o V_s / eN_d)$, where W is the thickness of the space-charge layer, ε is the static dielectric constant of the semiconductor, ε_o is the static dielectric constant in a vacuum, V_s is the surface potential, N_d is the number of dopant donor atoms, and e is the electron charge [78]. As the concentration of the dopant increases, the space-charge region becomes narrower and the electron hole pairs within the region are efficiently separated by the large electric field before recombination. However, when the concentration of doping is high, the space-charge region is very narrow so the penetration depth of light into TiO_2 greatly exceeds the width of the space-charge layer. Therefore, the rate of recombination of photogenerated electron- hole pairs in the semiconductor increases because there is no driving force to separate them. Consequently, there is an optimum concentration of dopant ions where the thickness of the space-charge layer is similar to the depth of light penetration.

Khan et al. [157] synthesized TiO_2 nanotubes hydrothermally and doped them with ruthenium using an ion exchange method. The resulting photocatalyst was active under visible light, exhibiting higher photocatalytic activity (>80%) for the degradation of methylene blue than undoped nanotubes. The loading method, size of ruthenium particles and metal dispersion pattern at the surfaces of the nanotubes had a great influence on their photocatalytic performance.

3.11.8 Addition of noble metals

Addition of noble metals is another approach for the modifying photocatalysts. Noble metals including Pt, Ag, Au, Pd, Ni, Rh and Cu have been reported to be very effective at enhancing photocatalysis by TiO_2. Because the Fermi levels of these noble metals are lower than that of TiO_2, photoexcited electrons can be transferred from the conduction band of TiO_2 to metal particles deposited on the surface of TiO_2, while photogenerated holes in the valence band remain on TiO_2. This greatly reduces the possibility of electron-hole recombination, resulting in efficient separation and higher photocatalytic activity. Numerous studies have found that the properties of these kinds of composites depend strongly on the size of the metal particle, dispersion and composition. When the size of the metal particles is less than 2.0 nm, the composites display exceptional catalytic behavior. It has been suggested that too high a concentration of metal particles reduces photon absorption by TiO_2 and allows the metal particles to become electron-hole recombination centers, resulting in lower efficiency.

Rupa et al. [158] synthesized TiO_2 nanoparticles by the sol-gel technique and doped the nanoparticles with about 1% noble metal (M/TiO_2, M = Ag, Au, and Pt) through photodeposition. M/TiO_2 catalysts showed remarkable photocatalytic activity towards the decolorization of tartrazine even under visible irradiation. The order of the photocatalytic activity of the different catalysts was:
$Au/TiO_2 > Ag/TiO_2 > Pt/TiO_2 >$ Synthesized $TiO_2 > TiO_2$(P-25 Degussa).

Papp et al. [159] found that the addition of palladium to TiO_2 powder by either photodecomposition or thermal decomposition increased its photocatalytic activity towards the degradation of 1,4-dichlorobenzene.

Wong et al. [160] observed that visible light induced H_2 production from an aqueous methanol solution over a Cu-ion doped TiO_2 photocatalyst.

More recently, Wu and Lee [161] reported that deposition with Cu particles greatly enhanced the photocatalytic activity of TiO_2 for producing H_2 from aqueous methanol solution.

3.11.9 Non metal co-doping

Doping with nonmetals like nitrogen, fluorine, chlorine, sulfur, boron and carbon in TiO_2 has been experimented. These nonmetals make TiO_2 efficient visible light active. The visible light efficiency increases manifold upon co-doping titania with these nonmetals. TiO_2 has been co-doped with N and S, N and F, and also N and B. A marked improvement in the visible light efficiency of the co-doped TiO_2 occurs in comparison to pure and single nonmetal doped titania due to the synergetic effect of the two nonmetals. Compared to pure titania, S- TiO_2 and N–TiO_2 films, N–S codoped TiO_2 films showed much higher hydrophilicity not only under visible light but also under fluorescent light (UV–vis both). The simultaneous substitution of N and S for O sites in TiO_2 results in hybridization of N 2p and S 3p bands generated close to the valence band edge which increases hydrophilicity and enhances hole mobility. Visible light degradation of methyl orange was increased by an increase in oxygen vacancies due to N doping and surface acidity by physically adsorbed S in N–S co-doped TiO_2 samples. Simultaneous substitution of N and S narrowed the band gap of TiO_2 and enhanced UV–vis absorption. In N–F co-doped TiO_2, nitrogen doped either substitutionally or as NO_x increased the visible light absorption while fluorine either substitutionally doped or physically adsorbed at the surface increased the surface acidity, hydroxyl radical formation and active surface sites generation.

In et al. [162] found no synergy in the B–N co-doped TiO_2 samples since they showed the same activity under visible light as B-only doped samples. Ling et al. [163] observed synergetic effect of both B and N atoms in co-doped titania. Doping B and N simultaneously narrowed the band gap of titania by modifying electronic structure around the conduction band edge and also increased visible light absorption.

3.11.10 Codoping of metal, non-metal and metal, metal

Codoping of TiO_2 may be used as an effective way to improve charge separation. Yang et al. [164] reported that monocrystalline TiO_2 codoped with optimal concentrations of Eu^{3+} and Fe^{3+} (1% Fe^{3+} and 0.5% Eu^{3+}) showed significantly enhanced photocatalytic activity compared with undoped TiO2. Fe^{3+} serves as a hole trap and Eu^{3+} as an electron trap, increasing the rates of anodic and the cathodic processes via improved interfacial charge transfer.

Vasiliu et al. [165] reported that Fe- and Eu-doped TiO_2 showed a red shift in its absorption spectrum and high photoactivity for the degradation and catalytic oxidation reactions of styrene

and phenol, respectively, when exposed to visible light.

Song et al. [166] prepared (Cu, N)-codoped TiO_2 nanoparticles and investigated the influence of the amounts of Cu and N codoped into TiO_2 on the photocatalytic activity. Codoping of TiO_2 with N and Cu extended absorption upto 590 nm and gave higher photocatalytic activity than pure N or Cu-doped TiO_2 for the photocatalytic degradation of xylenol orange, thus revealing a potential application in degrading organic pollutants.

Shen et al. [167] prepared a (N, Ce)-codoped TiO_2 photocatalyst by the sol-gel route that could degrade nitrobenzene under irradiation with visible light. Nitrogen atoms were incorporated into the TiO_2 crystal structure and narrowed the band gap energy. The dopant cerium atoms existed in the form of Ce_2O_3, and were dispersed on the surface of TiO_2. The improvement in the photocatalytic activity was ascribed to the synergistic effects of nitrogen and cerium codoping.

Yang et al. [168] codoped TiO_2 with metallic silver and vanadium oxide using a one-step sol-gel solvothermal method in the presence of a triblock copolymer surfactant (P123). The resulting Ag/V-TiO_2 three-component junction system exhibited the highest photocatalytic activity for the degradation of rhodamine B and Coomassie Brilliant Blue G-250 under both visible and UV light exceeding that of Degussa P25, pure TiO_2, singly-doped TiO_2 (Ag/TiO_2 or V-TiO_2) as well as a P123-free-Ag/V-TiO_2 codoped system.

3.12 Doped and coupled TiO_2

From the above discussion, it is clear that doping of TiO_2 can enhance its visible light activity significantly by changing the position of the conduction or valance bands by introducing impurity energy levels. The coupling of TiO_2 with other narrow band gap semiconductors could also enhance its visible light activity because electrons or holes photogenerated in the narrow band gap materials could be injected into TiO_2, resulting in better charge separation in the illuminated photocatalyst by enhancing the lifetimes of the e^- and h^+. To further improve the photocatalytic performance, various attempts have been made to study the combined effect of coupling and doping.

Zhang et al. [169] fabricated a photoelectrode photocatalyst that was active under visible light by modifying TiO_2 nanotubes with CdS and S^{6+}. S^{6+} doping narrowed the band gap to enhance the visible light response of TiO_2 and reduced the potential of the conduction band of TiO_2, accelerating the electron transfer between TiO_2 and CdS. The free energy (ΔG) for electron transfer between a donor and acceptor is a useful predictor of the activity of a coupled photocatalyst. ΔG for electron transfer between S-doped TiO_2 and CdS was determined according to the following equation: $\Delta G = -F (E_0 (S–TiO2(x)) – E_0 (CdS))$, where F is Faraday's constant (96486 C/mol), E_0 (CdS) and E_0 (S–TiO2(x)) are the standard reduction potentials of the conduction band electrons of CdS and S−TiO2(x), respectively, and "x" denotes the concentration of S^{6+}. Increasing the concentration of S^{6+} caused ΔG to decrease, suggesting that electron transfer between TiO_2 and CdS occurred more readily so the amount of carriers is increased, enhancing the photoactivity. Consequently, it was concluded that decreasing ΔG was one of the reasons for the high activity of CdS/S−TiO_2(x). Thus, by such modification, a promising photocatalyst can be produced.

Kumar and Jain [170] investigated the effect of addition of metal ions on the photoactivity of CdS-TiO_2 composite photocatalysts. Doping either $Cd(OH)_2$-coated Q-CdS or

TiO_2 with Ag^+ prior to their coupling (Ag^+-doped $Cd(OH)_2$-coated Q-CdS coupled with TiO_2 and Ag^+-doped TiO_2 coupled with $Cd(OH)_2$-coated Q-CdS) produced a three component composite catalyst [CdS-TiO_2-Ag_2S] system. The presence of Ag^+ in the TiO_2 lattice promoted the charge separation by scavenging shallowly trapped electrons from the conduction band of CdS and causing the trapped holes to move to deeper traps. The Ag-doped coupled photocatalyst system was found to be about twice as photocatalytically efficient as the undoped Q-CdS-TiO_2 composite for performing synthetic photochemistry.

4. Current and future developments

The current problem with doped TiO_2 may be the loss of photoactivity during recycling and long-term storage. It was assumed, that the efficiency of metal doped-TiO_2 under visible light strongly depended on the preparation method used. In same cases, such doped photocatalysts showed no activity under visible light and/or lower activity in the UV spectral range compared to the non-doped TiO_2 because of high carrier recombination rates through the metal ion levels.

The main present problem with nonmetal-doped TiO_2 photocatalyst is that the photocatalytic activity under visible light is much lower than that under ultraviolet light. Therefore, development of new and optimization of existing photocatalyts exhibiting activity upon visible light with surface characteristics of improved performance and of the high chemical and physical stability are crucial for broader scale utilization of photocatalytic systems in commercial application. Such materials together with the development of technically applicable self aligning photocatalytic coating systems adaptable to the major substrates (polymers, glass, ceramics or metals) will represent a ground breaking step change in this field particularly in the economic viability of a range of potential processes. Non metal doping seems to be more promising than metal doped- TiO_2.

One of the major challenges for the scientific and industrial community involved in photocatalytic research is to increase the spectral sensitivity of TiO_2-based photocatalysts to visible light. A major area of future research would be the development of new dopants, new method of dopant incorporation into TiO_2 structure as well as new application for environmental technology. Future patents would deal with visible light-activated TiO_2 functioning in the presence of solar irradiation. The most important challenge which faces titania-based catalysis is stable TiO_2 with predictable photoactivity in UV and visible light.

5. References

1. A. Fujishima, K. Honda, Nature., 1972, 238, 37.
2. P. V. Kamat, Chem. Rev., 1993, 93, 267.
3. A. Hagfeldt, M. Gratzel, Chem. Rev., 1995, 95, 49.
4. M. R. Hoffmann, S. T. Martin, W. Y. Choi, D. W. Bahnemann, Chem. Rev., 1995, 95, 69.
5. A. L. Linsebigler, G. Q. Lu, J. T. Yates, Chem. Rev., 1995, 95, 735.
6. D. Li, H. Haneda, N.K. Labhsetwar, S. Hishita, N. Ohashi, Chem. Phys. Lett., 2005, 401, 579–584.
7. M. Miyauchi, A.Nakajima, T.Watanabe, K. Hashimoto, Chem. Mater., 2002, 14, 2812–2816.
8. V. Srikant, D.R. Clarkea, J. Appl. Phys., 1998, 83, 5447–5451.
9. O. Carp, C.L. Huisman, A Reller, Prog in Solid State Chem., 2004, 32, 33–117
10. Y. P. Simons, F. Dachille, Acta Cryst., 1967, 23, 334–336

11. M. Latroche, L. Brohan, R. Marchand, J Solid State Chem., 1989, 81, 78–82
12. D. T. Cromer, K. Herrington, J Am Chem Soc., 1955, 77, 4708–4709
13. V. W. H. Baur, Acta Crystallogr., 1961, 14, 214–216
14. Mo S, W. Ching, Phys Rev B., 1995, 51, 13023–13032
15. Chen X, Mao S S., Chem Rev., 2007, 107, 2891–2959
16. Thompson T L, Yates Jr J T, Chem Rev., 2006, 106, 4428–4453
17. Diebold U, Sur Sci Rep., 2003, 48, 53–229
18. Norotsky A, Jamieson J C, Kleppa O J, Science., 1967, 158, 338–389
19. Zhang Q, Gao L, Guo J, Appl Catal B Environ., 2000, 26, 207–215
20. Sclafani A, Palmisano L, Schiavello M, J Phys Chem, 1990, 94, 829–832
21. Linsebigler A L, Lu G, Yates J T, Chem Rev., 1995, 95,735–758
22. Muscat J, Swamy V, Harrison N M, Phy Rev B., 2002, 65, 1–15
23. Tanaka K, Capule M F V, Hisanaga T, Chem Phys Lett, 1991, 187, 73–76
24. Selloni A, Nature Mater., 2008, 7, 613–615
25. Yang H G, Sun C H, Qiao S Z, Nature., 2008, 453, 638–641
26. P. Suppan, Royal Society of Chemistry, Cambridge, 1994.
27. A. Testino, I. R. Bellobono, V. Buscaglia, C. Canevali, M. D'Arienzo, S. Polizzi, R. Scotti, F. Morazzoni, J. Am. Chem. Soc., 2007, 129, 3564-3575
28. A. Mills, S. Le Hunte, J. Photochem. Photobiol. A., 1997, 108, 1-35
29. Y. Li, D.-S. Hwang, N. H. Lee, S.-J. Kim, Chem. Phys. Lett., 2005, 404
30. J. Yu, H. Yu, B. Cheng, M. Zhou, X. Zhao, J. Mol. Catal A., 2006, 253
31. C. A. Emilio, M. I. Litter, M. Kunst, M 1 . Bouchard, C. Colbeau, Langmuir., 2006, 22, 3606-3613
32. W. Choi, A. Termin, M. R. Hoffmann, J. Phys. Chem. B., 1994, 98, 13669-13679
33. T. Tachikawa, M. Fujitsuka, T. Majima, J. Phys. Chem. C., 2007, 111, 5259-5275
34. A. Hoffman, E. R. Carraway, M. Hoffman, Environ. Sci. Technol., 1994, 28, 776- 785.
35. M.D. Hernandez-Alonso, F. Fresno, S. Suarez, J.M. Coronado, Energy Environ. Sci., 2009, 2, 1231-1257
36. A. Sclafani, J. Phys. Chem., 1996, 100, 13655-13661
37. X. Chen, S. S. Mao, Chem. Rev., 2007, 107, 2891-2959
38. J. Liqiang, Q. Yichun, W. Baiqi, L. Shudan, J. Baojiang, Y. Libin, F. Wei, F. Honggang, S. Jiazhong, Solar Energy Materials & Solar Cells., 2006, 90, 1773- 1787
39. N. Serpone, J. Photochem. Photobiol. A., 1997, 104
40. J. Yu, H. Yu, B. Cheng, M. Zhou, X. Zhao, J. Mol. Catal. A., 2006, 253
41. You X, Chen F, Zhang J, J Sol-Gel Sci Tech., 2005, 3, 181–187
42. Hu Y, Tsai H L, Huang C L, Mater Sci Eng A., 2003, 344, 209–214
43. Wang J, Li R H, Zhang Z H, Inorg Mater., 2008, 44, 608–614
44. Ohtani B, Ogawa Y, Nishimoto S, J Phys Chem B., 1993, 101, 3746–3752
45. Yu J, Zhao X, Zhao Q, Mater Chem Phys., 2001, 69, 25–29
46. Miller R J D, McLendon G L, Nozik A J, Surface Electron-transfer Processes, New York, VCH, 1995
47. D. Chatterjee, A. Mahata, Catal. Commun., 2001, 2, 1–3
48. D. Chatterjee, A. Mahata, J. Photochem. Photobiol. A: Chem., 2002, 153, 199–204
49. J. Zhao, C. Chen,W. Ma, Top. Catal., 2005, 35, 269–278

50. R. Abe, K. Hara, K. Sayamaa, K. Domen, H. Arakawa, J. Photochem. Photobiol. A: Chem., 2000, 137 63–69
51. S. Kaur,V. Singh, Ultrason. Sonochem., 2007, 14, 531–537
52. J. Moon, C.Y. Yun, K.-W. Chung, M.-S. Kang, J. Yi, Catal. Today., 2003, 87, 77–86
53. Nishikiori H, Qian W, El-Sayed M A, J Phys Chem C Lett., 2007, 111, 9008–9011
54. Benko G, Skarman B, Wallenberg R, J Phys Chem B., 2003, 107, 1370–1375
55. Li X Z, Zhao W, Zhao J C, Sci China Ser B-Chem, 2002, 45, 421–425
56. D. Jiang, Y. Xu, B. Hou, D. Wu, Y. Sun, J. Solid State Chem., 2007, 180, 1787–1791
57. M. Li, P. Tang, Z. Hong, M. Wang, Colloids Surf. A: Physicochem. Eng. Aspects., 2008, 318, 285–290
58. D. Jiang, Y. Xu, D.Wu, Y. Sun, J. Solid State Chem., 2008, 181, 593–602
59. L. Song, R. Qiu, Y. Mo, D. Zhang, H. Wei, Y. Xiong, Catal. Commun., 2007, 8, 429–433
60. R. Qiu, D. Zhang, Y. Mo, L. Song, E. Brewer, X. Huang, Y. Xiong, J. Hazard. Mater., 2008, 156, 80–85
61. Y. Bessekhouad, D. Robert, J.V. Weber, J. Photochem. Photobiol. A: Chem., 2004, 163, 569–580
62. L.Wu, J.C. Yu, X. Fua, J. Mol. Catal. A: Chem., 2006, 244, 25–32
63. S.M. Ji, H. Jun, J.S. Jang, H.C. Son, P.H. Borse, J.S. Lee, J. Photochem. Photobiol. A: Chem., 2007, 189, 141–144
64. W. Ho, J.C. Yu, J. Mol. Catal. A: Chem., 2006, 247, 268–274
65. L. Jianhua, Y. Rong, L. Songmei, Rare Met., 2006, 25, 636–642
66. I. Nakamura, N. Negishi, S. Kutsuna, T. Ihara, S. Sugihara, K. Takeuch, J. Mol. Catal. A: Chem., 2000, 161, 205–212
67. T. Ihara, M. Miyoshi, Y. Iriyama, O. Matsumoto, S. Sugihara, Appl. Catal. B: Environ., 2003, 42, 403–409
68. I. Justicia, G. Garcia, G.A. Battiston, R. Gerbasi, F. Ager, M. Guerra, J. Caixach, J.A. Pardo, J. Riverad, A. Figueras, Electrochim.Acta., 2005, 50, 4605–4608
69. Y-C. Nah, I. Paramasivam, P. Schmuki, Chem. Phys. Chem., 2010, 11, 2698
70. N. Serpone, J. Phys. Chem. B., 2006, 110, 24287-24293
71. X. Chen, L. Liu, P. Y. Yu, S. S. Mao, Science., 2011, 331, 746-750
72. Zhang L W, Fu H B, Zhu Y F, Adv Funct Mater., 2008, 18, 2180–2189
73. Zhang L W, Wang Y, Xu T, J Mol Cataly A: Chem., 2010, 331, 7–14
74. Takeuchi M, Sakai S, Ebrahimi A, Top Cataly., 2009, 52, 1651–659
75. Rajeshwar K, de Tacconi N R, Chenthamarakshan C R, Chem Mater, 2001, 13, 2765–2782
76. Gerischer H, J Electroanal Chem., 1977, 82, 133–143
78. Sung Y M, Lee J K, Chae W S, Crystal Growth Design., 2006, 6, 805–808
79. Liz-Marzan L M, Mulvaney P, J Phys Chem B., 2003, 107, 7312–7326
80. Hirakawa T, Kamat P V, Langmuir., 2004, 20, 5645–5647
81. Comparelli R, Fanizza E, Curri M L, Appl Catal B, 2005, 55, 81–91
82. Fittipaldi M, Curri M L, Comparelli R, J Phys Chem C., 2009, 113, 6221–6226
83. C. Aprile, A. Corma, H. Garcia, J. Phys. Chem., 2008, 10, 769–783
84. S.H. Bossmann, S. Jockusch, P. Schwarz, B. Baumeister, S. Gob, C. Schnabel, L. Payawan Jr., M.R. Pokhrel, M. Worner, A.M. Braun, N.J. Turro, Photochem. Photobiol. Sci., 2003, 2, 477–486.

85. S.H. Bossmann, C. Turro, C. Schnabel, M.R. Pokhrel, L.M. Payawan Jr., B. Baumeister, M. Worner, J. Phys. Chem. B., 2001, 105, 5374–5382
86. M. Alvaro, E. Carbonell, V. Fornes, H. Garcia, Chem Phys Chem., 2006, 7, 200–205
87. S. Klosek, D. Raftery, J. Phys. Chem. B., 2001, 105, 2815-2819
88. A. Kudo, R. Niishiro, A. Iwase, and H. Kato, Chem Phys., 2007, 339, 1-3
89. X.Wang, S.Meng, X. Zhang, H.Wang,W. Zhong, Q. Du, Chem. Phys. Let., 2007, 444, 4-6.
90. E. Setiawati, K. Kawano, J. Alloys and Compounds., 2008, 451, 293-296
91. X. Fan, X. Chen, S. Zhu, J. Molecular Catalysis A., 2008, 284, 155-160
92. A. Kubacka, G. Colon, M. Fernandez, Catalysis Today., 2009, 143, 286-292
93. H. Cai, G. Liu, W. L¨u, X. Li, L. Yu, D. Li, J. Rare Earths., 2008, 26, 71-75
94. E. Setiawati, K. Kawano, Journal of Alloys and Compound.s, 2008, 451, 293-296
95. Asahi R, Morikawa T, Ohwaki T, Aoki K, Taga Y, Science., 2001, 293, 269-271
96. Irie H, Watanabe Y, Hashimoto K, J Phys Chem B., 2003, 5483-5486.
97. Ihara T, Miyoshi M, Triyama Y, Marsumato O, Sugihara S, Appl Catal B., 2003, 42, 403-409
98. S. Sato, Chem. Phys. Lett., 1986, 123, 126-128
99. S. Sato, R. Nakamura, S. Abe, Appl. Catal. A: General., 2005, 284, 131-137
100. R. Asahi, T. Morikawa, T. Ohwaki, K. Aoki, Y. Taga, Science., 2001, 293, 269-271
101. N. Serpone, J. Phys. Chem. B., 2006, 110, 24287-24293
102. C. Di Valentin, E. Finazzi, G. Pacchioni, A. Selloni, S. Livraghi, M. C. Paganini, E. Giamello, Chem. Phys., 2007, 339, 44-56
103. S.U.M. Khan, M. Al-Shahry, W.B. Ingler, Science., 2002, 297, 2243-2245
104. Y. Izumi, T. Itoi, S. Peng, K. Oka, Y. S 1 hibata, J. Phys. Chem. C., 2009, 113, 6706-6718
105. J. Zhang, Y. Wu, M. Xing, S.A.K. Leghari, S. Sajjad, Energy Environ. Sci., 2010, 3, 715-726
106. Y. Nakano, T. Morikawa, T. Ohwaki, Y. Yaga, Appl. Phys. Lett., 2005, 86, 130-132
107. J.M. Mwabora, T. Lindgren, E. Avendano, T.F. Jaramillo, J. Lu, S.E. Lindqusit, C.G. Granqvist, J. Phys. Chem. B., 2004, 108, 20193-20198
108. S-H. Lee, E. Yamasue, H. Okumura, K.N. Ishihara, Appl. Catal. A: General., 2009, 371, 179-190
109. E. Martínez-Ferrero, Y. Sakatani, C. Boissière, D. Grosso, A. Fuertes, J. Fraxedas, C. Sanchez, Adv. Funct. Mater., 2007, 17, 3348-3354.
110. G. Abadias, F. Paumier, D. Eyidi, P. Guerin, T. Girardeau, Surf. Interf. Anal., 2010, 42, 970-973
111. J. Premkumar, Chem. Mater., 2006, 16, 3980-3981
112. Li Jinlong, M. Xinxin, S. Mingren, X. Li, S. Zhenlun, Thin Solid Films., 2010, 519, 101-105.
113. A. Kafizas, C. Crick, I. P. Parkin, J. Photochem. Photobiol. A: Chem., 2010, 216, 156-166
114. C.W.H. Dunnill, Z. A. Aiken, J. Pratten, M. Wilson, D. J. Morgan, I. P. Parkin, J. Photochem. Photob. A: Chem., 2009, 207, 244-253
115. C. Sarantopoulos, A. N. Gleizes, F. Maury, Thin Solid Films., 2009, 518, 1299- 1303
116 72. V. Pore**,** M. Heikkilä**,** M. Ritala**,** M. Leskelä, S. Arev**,** J. Photochem. Photob. A: Chem., 2006, 177, 68-75
117. L. Zhao, Q. Jiang, J. Lian, Appl. Surf. Sci., 2008, 254, 4620-4625
118. D. Mitoraj, H. Kisch, Chem. Eur. J., 2010, 16, 261-269

119. T.C. Jagadale, S. P. Takale, R.S. Sonawane, H.M. Joshi, S.I. Patil, B. Kale, S. B. Ogale, J. Phys. Chem. C., 2008, 112, 14595-14602
120. X. Qiu, Y. Zhao, C. Burda, Adv. Mater., 2007, 19, 3995-3999
121. T. Sano, N. Negishi, K. Koike, K. Takeuchi, S. Matsuzawa, J. Mater. Chem., 2004, 14, 380-384
122. C. Belver, R. Bellod, A. Fuerte, M. Fernandez-Garcia, Appl. Catal. B: Environ., 2006, 65, 301-308
123. A. I. Kontos, A. G. Kontos, Y. S. Raptis, P. Falaras, Phys. Stat. Sol., 2008, 2, 83-85
124. H. Choi, M. G. Antoniou, M. Pelaez, A. A. de la Cruz, J. A. Shoemaker, D. D. Dionysiou, Environ. Sci. Technol., 2007, 41, 7530-7535
125. H. Choi, A. C. Sofranko, D. D. Dionysiou, Adv. Funct. Mater., 2006, 16, 1067- 1074
126. H. Choi, E. Stathatos, D. D. Dionysiou, Appl. Catal. B., 2006, 63, 60-67
127. X. Fang, Z. Zhang, Q. Chen, H. Ji, X. G. J. Solid State Chemistry., 2007, 180, 1325-1332
128. F.E. Oropeza, J. Harmer, R. G. Egdell, R. G. Palgrave, Phys. Chem. Chem. Phys., 2010, 12, 960-969
129. Y. Irokawa, T. Mor 1 ikawa, K. Aoki, S. Kosaka,T. Ohwaki,Y. Taga, Phys. Chem. Chem. Phys., 2006, 8, 1116-112
130. D.J.V. Pulsipher, I. T. Martin, E.R. Fisher, Appl. Mat. Interf., 2010, 2, 1743-1753
131. V. Etacheri, M. K. Seery, S. J. Hinder, S. C. Pillai, Chem. Mater., 2010, 22, 3843- 3853
132. Q. Li, J. K. Shang, J. Am. Ceram. Soc., 2008, 91, 3167-3172
133. J. Wang, De N. Tafen, J. P. Lewis, Z. Hong, A. Manivannan, M. Zhi, M. Li, N. Wu, J. Am. Chem. Soc., 2009, 131, 12290-12297
134. R.P. Vitiello, J. M. Macak, A. Ghicov, H. Tsuchiya, L. F. P. Dick, P. Schmuki, Electrochem. Commun., 2006, 8, 544-548
135. A. Ghicov, J-M. Macak, H. Tsuchiya, J. Kunze, V. Haeublein, L. Frey, P. Schmuki, Nano Lett., 2006, 6, 1080-1082
136. K.S. Han, J.W. Lee, Y.M. Kang, J.Y. Lee, J.K. Kang, Small., 2008, 4, 1682-1686
137. J. Wang, Z. Wang, H. Li, Y. Cui, Y. Du, J. Alloys Comp., 2010, 494, 372-377
138. C. Liu, H. Sun, S. Yang, Chem. Eur. J., 2010, 16, 4381-4393
139. K. Shankar, K. C. Tep, G.K. Mor, C.G. Grimes, J. Phys. D: Appl. Phys., 2006, 39, 2361-2366
140. D. Wu, M. Long, W. Caia C. Chen, Y. Wu, J. Alloys Comp., 2010, 502, 289-294
141. G. Liu, L. Wang, C. Sun, Z. Chen, X. Yan, L. Cheng, H-M. Cheng, G.Q. Lu, Chem. Commun., 2009, 1383-138
142. J.C. Yu, J. Yu,W. Ho, Z. Jiang, L. Zhang, Chem. Mater., 2002, 14, 3808–3816
143. N. Todorova, T. Giannakopoulou, G. Romanos, T. Vaimakis, J. Yu, C. Trapalis, Int. J. Photoenergy., 2008, 1-9
144. T. Yamaki, T. Umebayashi, T. Sumita, S. Yamamoto,M. Maekawa, A. Kawasuso, H. Itoh, Nucl. Instrum. Methods Phys. Res. B., 2003, 206, 254–258
145. G.Wu, A. Chen, J. Photochem. Photobiol. A: Chem., 2008, 195, 47–53
146. L. Mingce, C.Weimin, C. Heng, X. Jun, Front. Chem. China., 2007, 2(3), 278–282
147. Y. Xie, Y. Li, X. Zhao, J. Mol. Catal. A: Chem., 2007, 277, 119-126
148. S. Liu, J. Yu, W. Wang, Phys. 1 Chem. Chem. Phys., 2010, 12, 12308-12315
149. S. In, A. Orlov, R. Berg, F. Garcıa, S. Pedrosa-Jimenez, M.S. Tikhov, D.S.Wright, R.M. Lambert, J. Am. Chem. Soc., 2007, 129, 13790–13791

150. X. Zhang, Q. Liu, Mater. Lett., 2008, 62, 2589–2592
151. C. Xu, R. Killmeyer, M.L. Gray, S.U.M. Khan, Appl. Catal. B: Environ., 2006, 64, 312–317
152. W. Ren, Z. Ai, F. Jia, L. Zhang, X. Fan, Z. Zou, Appl. Catal. B: Environ., 2007, 69, 138–144
153. M.-S. Wong, S.-W. Hsu, K.K. Rao, C.P. Kumar, J. Mol. Catal. A: Chem., 2008, 279, 20–26
154. S. Sakthivel, H. Kisch, Angew. Chem. Int. Ed., 2003, 42, 4908–4911
155. Grätzel M, Howe R F, J. Phys. Chem., 1990, 94, 2566–2572
156. Joshi M M, Labhsetwar N K, Mangrulkar P A, App Catal A General., 2009, 357, 26–33
157. Khan M A, Han D H, Yang O B, Appl Surf Sci., 2009, 255, 3687–3690
158. Rupa A V, Divakar D, Sivakumar T, Catal Lett., 2009, 132, 259–267
159. Papp J, Shen H S, Kershaw R, Chem Mater., 1993, 5, 284–288
160. Wong W K, Malati M A, Sol Energy., 1986, 36, 163–168
161. Wu N L, Lee M S, Inter J Hydro Energ., 2004, 29, 1601–1605
162. S. In, A. Orlov, R. Berg, F. Garcıa, S. Pedrosa-Jimenez, M.S. Tikhov, D.S.Wright, R.M. Lambert, J. Am. Chem. Soc., 2007,129, 13790–13791
163. Q. Ling, J. Sun, Q. Zhou, Appl. Surf. Sci., 2008, 254, 3236–3241
164. Yang P, Lu C, Hua N, Mater Lett., 2002, 57, 794–801
165. Vasiliu F, Diamandescu L, Macovei D, Top Catal., 2009, 52, 544–556
166. Song K, Zhou J, Bao J, J Am Ceram Soc., 2008, 91, 1369–1371
167. Shen X Z, Liu Z C, Xie S M, J Hazard Mater., 2009, 162, 1193–1198
168. Yang X, Ma F, Li K, J Hazard Mater., 2010, 175, 429–438
169. Zhang X, Lei L, Zhang J, Separ Purif Tech., 2009, 66, 417–421
170. Kumar A, Jain A K, J Mol Catal A Chem., 2001, 165, 265–273